This is the accepted manuscript of the article that appeared in final form in **Colloids and Surfaces B: Biointerfaces** 159 : 30-38 (2017), which has been published in final form at https://doi.org/10.1016/j.colsurfb.2017.07.081. © 2017 Elsevier under CC BY-NC-ND license (http://creativecommons.org/licenses/by-nc-nd/4.0/)

Synthesis and characterization of hyaluronic acid coated manganese dioxide microparticles that act as ROS scavengers

Joëlle Bizeau[a,b,†], Christos Tapeinos[a,†], Claudio Marella[a], Aitor Larrañaga[c], Abhay Pandit[a,*]

[a]*Centre for Research in Medical Devices (CÚRAM), National University of Ireland Galway, Galway, Ireland.*

[b]*National Polytechnic Institute of Chemical Engineering and Technology (ENSIACET), 4 allée Emile Monso, Toulouse, France*

[c]*Department of Mining-Metallurgy Engineering and Materials Science & POLYMAT, University of the Basque Country, Bilbao, Spain*

[†]These authors contributed equally to this work

*Corresponding author

joelle.bizeau@ensiacet.fr, ctapeinos@gmail.com, aitor.larranagae@ehu.eus, c.marella1@nuigalway.ie, abhay.pandit@nuigalway.ie

Graphical Abstract

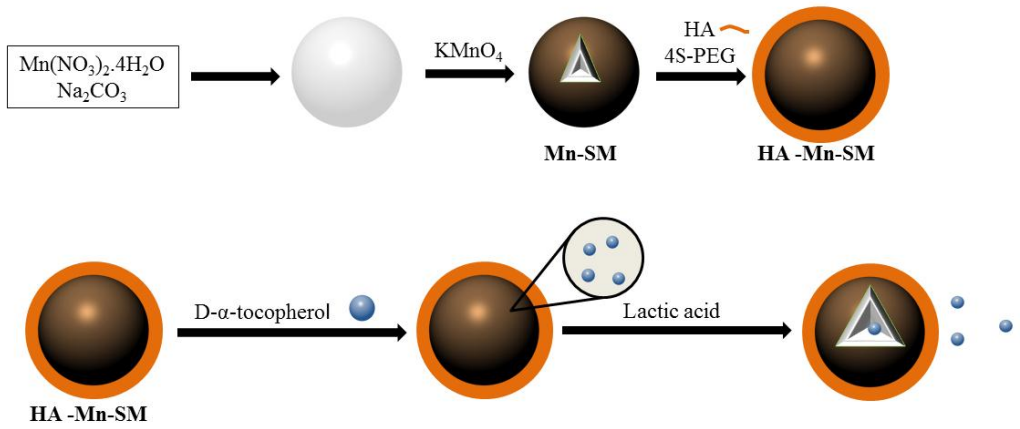

Highlights

- Synthesis of hyaluronic acid-coated manganese dioxide microspheres (HA-Mn-SM) with ROS scavenging ability
- The HA-Mn-SM scavenge H_2O_2 and generate O_2 in a controlled manner
- The HA-Mn-SM can be loaded with anti-oxidant substances and their release is dependent on lactic acid concertation
- The HA-coated microspheres are not cytotoxic
- The developed platform can be used as a DDS for the targeted delivery of anti-oxidants in atherosclerotic tissues

Abstract

Atherosclerosis is a chronic inflammatory disease of the arterial wall that leads to cardiovascular diseases which are the major cause of deaths worldwide. There is currently no treatment that can stop or reverse the disease. However, the use of microparticles with anti-inflammatory properties could represent a promising treatment. Herein, spherical microparticles with a core-shell structure and an average diameter of 1 µm were synthesized. The microparticles were comprised of a $MnCO_3$ and MnO_2 core and a 4-arm PEG-amine cross-linked shell of hyaluronic acid. The HA-Mn-SM microparticles were loaded with D-α-tocopherol (vitamin-E) (TOC), to fabricate a targeted biocompatible delivery platform for the treatment of atherosclerotic inflamed cells. Loading and release studies of TOC demonstrated a lactic acid concentration dependant controlled release profile of the HA-Mn-SM mimicking the atherosclerotic environment where lactic acid is over-produced. The microparticles exhibited a high

ACCEPTED MANUSCRIPT

scavenging ability towards H_2O_2 in addition to the controlled generation of O_2. The optimal results were obtained for 250 μg/mL microparticles which in the presence of 1000 μM H_2O_2 resulted in the scavenging of almost all the H_2O_2. Our results demonstrate that 50 μg/mL of microparticles scavenged continuously produced H_2O_2 up to a concentration of 1000 μM, a characteristic that demonstrates the sustained therapeutic effect of the HA-Mn-SM microparticles in an environment that mimics that of inflamed tissues. Our results indicate the potential use of HA-Mn-SM as a novel platform for the treatment of atherosclerosis. *In vitro* studies confirmed that the microparticles are not cytotoxic at concentrations up to 250 μg/mL and for 72 hours. These preliminary results indicate the potential use of HA-Mn-SM as a novel drug delivery system for atherosclerotic tissues.

Keywords: **Atherosclerosis; drug delivery; manganese dioxide; microspheres; ROS scavenging**

Number of words: 6876
Number of Tables: 0
Number of Figures: 7

ACCEPTED MANUSCRIPT

1. Introduction

Atherosclerosis is a chronic inflammatory disease of the arterial wall that damages the endothelium that in turn initiates an inflammatory cascade which results in the accumulation of low-density lipoproteins (LDL) known as "bad" cholesterol. Inflammation leads to the overproduction of Reactive Oxygen Species (ROS) resulting in the oxidation of LDL. Oxidized LDL (OxLDL) is up taken by macrophages which accumulate in atherosclerotic tissues which along with other mechanisms [1, 2] contribute to the formation of atherosclerotic plaques which in turn results in the onset of cardiovascular diseases including coronary artery disease, cerebrovascular disease and peripheral artery disease [3, 4]. Cardiovascular diseases account for the highest percentages of morbidity and mortality worldwide. In the European Union 42% of all deaths in 2012 resulted from a disease of the circulatory system, while cancer (malignant neoplasms), the second most prevalent cause of death, accounted for only 24.8% of deaths. [5]. In the United States in 2013, one of every three deaths was caused by a cardiovascular disease. Every 34 seconds, someone suffered a coronary event and every 84 seconds, someone died from a coronary event [6]. To date, the treatments for atherosclerosis comprise mostly of preventive strategies that act on a person's lifestyle by reducing various risk factors including smoking and by promoting regular exercise notably to control the person's weight [3, 4, 7, 8]. Unfortunately, these actions cannot stop the progression or reverse the formation of atherosclerotic plaques. Another approach for the treatment of atherosclerosis includes the use of drugs such as a) statins that reduce LDL and increase high-density lipoproteins (HDL) [9, 10], b) anti-platelet medication [4, 8] and c) beta blocker medication [4, 8] that reduce heart rate and blood pressure. When these treatments fail to meet the required standards, more aggressive treatments including angioplasty and stent placement or endarterectomy can be applied. As mentioned before, one of the mechanisms that lead to atherosclerosis is the overproduction of ROS and the transformation of LDL to OxLDL. Although the above-mentioned treatments can delay the progression of atherosclerosis, they do not lead to its regression and one possible reason for this may be that they do not take into consideration the inflammatory environment of the disease.

Manganese dioxide (MnO_2) is a well-known catalyst for the decomposition of hydrogen peroxide ($H_2O_2$to water and oxygen. A number of studies have attempted to understand the mechanism of action [11] and to evaluate its efficacy as a catalyst in relation to the particles' size, shape and composition [12-15], and the rate of decomposition.

It has also been shown that MnO_2 nanoparticles react directly with H_2O_2 to produce water, oxygen and Mn^{2+} ions [16], and Mn^{2+} ions are found inside numerous biological systems [17]. In addition, it has been demonstrated that Mn^{2+} ions produce a protective effect against H_2O_2-mediated injuries in certain conditions [18].

To date, several stimuli-responsive drug delivery systems for the treatment of cancer have been developed [19-21] and even though the catalytic and reactive properties of MnO_2 micro- and nano-particles have been used largely for the development of biosensors and super capacitors [13, 22], their role as a drug delivery system (DDS) is just beginning to be investigated [22-26]. Liu et al developed a microchip in which microchannels are composed of a fluid layer of polydimethylsiloxane and a serpentine MnO_2 nanofiber substrate with an epithelial cell adhesion antibody coating. These microchips capture and release circulating tumor cells in order to measure and analyze them for diagnostic purposes [27]. In addition, manganese-based systems including MnO_2 nanoparticles have been used as imaging agents in various diseases [28-32].

Hyaluronic acid (HA) is a carbohydrate composed of D-Glucuronic acid and N-acetyl-D-glucosamine linked by alternating β-1, 4 and β-1, 3 glycosidic bonds which is found in the extracellular and pericellular matrix [33] as also inside cells. Its abundant presence in the body ensures the biocompatibility of this natural polymer, and its use as a coating material provides protection to the various micro- and nano- constructs from the immune system. Its main receptor, CD44 is not only overexpressed in various cancer tumour cells but also in inflammatory cells [34] including activated macrophages which play an important role in the development of atherosclerotic plaques [35]. In addition, Stabilin-2, another HA receptor, is highly expressed in atherosclerotic plaques [35]. The

ACCEPTED MANUSCRIPT

biocompatibility and biodegradability of HA, in addition to the he presence of its receptor in cancerous and inflamed tissues, renders it a suitable material for coating and targeted treatment applications. For these reasons, HA is used for the synthesis of HA nanoparticles [35] as well as a material for coating drug delivery systems including chitosan [36], liposomes [37] and nanostructured lipid carriers [38].
Even though the exact mechanism of action of vitamin-E as an anti-oxidant is not well understood, it is believed that it protects LDL from ROS oxidation [39] and that it modulates a variety of inflammatory processes [40] involved in atherogenesis. Furthermore, D-α-tocopherol (TOC), the most active form of vitamin-E, inhibits smooth muscle cell proliferation and downregulates monocyte recruitment and scavenger receptor CD36 expression, reducing the uptake of LDL by macrophages [41]. It also acts as an inhibitor of proinflammatory cytokines produced by endothelial and immune cells, and as a suppressor of the expression of adhesion molecules to endothelial cells. It also acts as a reductor of the attraction of monocytes to inflammatory sites at the arterial wall [39].
Taking into consideration the properties of all the above-mentioned materials, we synthesized and characterized a multifunctional drug delivery system that can be used as a potential treatment for atherosclerotic tissues. In this study, we present the synthesis of a new drug delivery system consisting of MnO_2 spherical microparticles coated with HA. This platform can act as a ROS scavenger due to the incorporation of MnO_2 spherical microparticles, and also provides a controlled release profile of an encapsulated drug following the dissolution of the microparticles in lactic acid, a substance that is overproduced in atherosclerotic tissues. We hypothesized that the combination of MnO_2 microparticles and D-α-tocopherol would inhibit the progression of atherosclerosis by reducing the excess of ROS and by inhibiting the oxidation of LDL and the subsequent uptake of oxidized LDL by the macrophages.

2. Materials and methods

2.1. Materials

Manganese (II) nitrate tetrahydrate ($Mn(NO_3)_2.4H_2O$), sodium carbonate (Na_2CO_3), potassium permanganate ($KMnO_4$), hydrogen peroxide (H_2O_2) and 2-(N-morpholino) ethane sulfonic acid (MES $C_6H_{13}NO_4S$) were used as received from Sigma-Aldrich. L-(+)-Lactic acid ($C_3H_6O_3$), sodium chloride NaCl and D-α-Tocopherol polyethylene glycol 1000 succinate (TOC) were used as received from Sigma Life Sciences. N-(3-dimethylaminopropyl)-N'-ethyl carbodiimide hydrochloride (EDC) and N-hydroxysuccinimide (NHS) were used as received from Fluka Analytical. 4-arm PEG amine(pentaerythritol)•HCl was used as received from JenKem Technology. A 10mg/mL hyaluronic acid solution was prepared by dissolving sodium hyaluronate (800kDa - 1.2MDa) received from Lifecore Biomedical in deionized water and stored at 4°C. Ethanol (C_2H_5OH) was used as received from Lennox.
For the *in vitro* studies, 3T3 fibroblastic cells from rats were used. Hank's Balanced Salt Solution (HBSS) and Dulbecco's Modified Eagle's Medium (DMEM) with and without Phenol Red were purchased from Sigma Life Sciences. Trypsin-EDTA was used as received from Sigma-Aldrich and AlamarBlue® was used as received from Life Technologies/Biosciences.

2.2. Characterization methods

The chemical composition of the spheres was verified using a Fourier Transform Infrared spectrometer Varian 660-IR. The transformation of the $KMnO_4$ into MnO_2 was studied using UV-Vis spectrophotometry (Varioskan Flash Spectral Scanning Multimode Reader with Skanit software 2.4.3 from Thermo Scientific) and X-Ray powder diffraction analysis (Inel Equinox 3000 X-ray powder diffractometer). The morphological characterization of the microparticles was carried out using a Scanning Electron Microscope (SEM) with EDX Analysis System, at a working voltage and working current of 5 kV and 10 mA respectively. ζ-potential was determined using Dynamic Light Scattering (Zetasizer Nano Series, Malvern Instrument). A Varioscan Flash UV-Vis plate reader was used for reading fluorescence to assess the H_2O_2 scavenging effect of the microparticles and the readouts were

ACCEPTED MANUSCRIPT

measured at λ_{ex}=540 nm/ λ_{em}=590 nm. Oxygen generation was measured using a Microx 4 trace fibre optic oxygen meter® with a PSt7-O_2 micro-sensor. Data was collected every two seconds for 60 minutes using the Data Manager software of Presens® and analyzed using OriginPro®.
Quantification of the amount of loaded TOC was carried out using Nuclear Magnetic Resonance (JEOL-400MHz NMR Instrument) of the hydrogen nucleus. During the washing of the spheres, the first supernatant was collected and frozen at -80 °C for 30 minutes before being transferred to the freeze dryer. Then, the sample was dissolved in deuterated DMSO. Four samples containing 0.5, 1.0, 1.5 and 2.0 mg/mL of TOC in deionized water were prepared as described to obtain the characteristic spectrum of the TOC and to plot a calibration curve using the integration of the peaks.

2.3. Synthesis of MnO_2 spherical microparticles (Mn-SM)

2.3.1. Preparation of $MnCO_3$ template

The $MnCO_3$ microparticles were synthesized according to a modified protocol previously reported [42]. Briefly, 20 mL of a 0.1 M $Mn(NO_3)_2{\cdot}4H_2O$ solution was added to 20 mL of a 0.1 M Na_2CO_3 solution with a flow rate of 10 mL/min under vigorous stirring. The solution turned milky white from the addition of the first drop suggesting the instant formation of manganese carbonate. After the addition of $Mn(NO_3)_2$, the stirring was stopped and the spheres were left for 15 minutes at room temperature before being washed three times with deionized water. The product was collected using centrifugation at 8000 rpm for 5 minutes. After the washings, the particles were dried and stored at room temperature.

2.3.2. Preparation of the MnO_2 microparticles

The MnO_2 microparticles were synthesized according to a modified protocol previously reported [43]. A molar ratio of $KMnO_4$ to $MnCO_3$) of 1 to 50 was used for the synthesis. 10 mL of the $KMnO_4$ solution was added to the $MnCO_3$ microparticles and the solution was stirred vigorously for 30 minutes. The solution turned brown and then the spheres were collected using centrifugation and washed four times with deionized water. The centrifugation used for this step was 8000 rpm for 5 minutes. After the washings, the particles were dried and stored at room temperature.

2.4. Coating of Mn-SM with Hyaluronic Acid (HA-Mn-SM)

30 mg of Mn-SM was suspended in 1.50 mL of a 0.15 M NaCl solution, (pH 6.5) under vigorous stirring. Then 0.5 mL of a 10 mg/mL HA solution was added. The solution was stirred for 30 minutes before being centrifuged at 4500 rpm for one minute to separate the particles from the liquid. The particles were washed three times with a 0.01 M NaCl solution (pH 6.5) before being dried and stored at room temperature.

2.5. Cross-linking with 4-arm-PEG-amine (4S-PEG)

30 mg of HA-Mn-SM microparticles, 15 mg of EDH and 15 mg of NHS were suspended in 4 mL of MES buffer at pH 6 and stirred for 30 minutes. Then the pH was increased with a 10 M NaOH solution to pH 7.4 before the addition of 5 mg of 4-arm PEG-amine dissolved in 1 mL of deionized water. The solution was stirred for 5 hours before being centrifuged at 8000 rpm for 5 minutes and washed five times with deionized water. The sample was then dried and stored at room temperature.

2.6. Effect of lactic acid in the HA-Mn-SM microparticles

The effect of lactic acid was tested on plain $MnCO_3$ microparticles and on HA-Mn-SM microparticles cross-linked with 4S-PEG. 10 mg of $MnCO_3$ microparticles was placed in 5 mL of lactic acid 0.01 M (pH 3) while stirring. Every 5 minutes the solution was changed with fresh lactic acid of the same concentration added in order to maintain a stable pH. This was done to simulate the continuous generation of lactic acid in the body. The same procedure was followed for the cross-linked HA-Mn-SM.

ACCEPTED MANUSCRIPT

2.7. Loading and Release studies using D-α-tocopherol

2.7.1. Loading by entrapment during the synthesis of $MnCO_3$ microparticles

The loading of TOC was carried out during the synthesis of $MnCO_3$ microparticles. 6 mg of TOC was dissolved in 1 mL of deionized water and 1 mL of a 0.1 M Na_2CO_3 solution was added under vigorous stirring. Then, 1 mL of a 0.1 M $Mn(NO_3)_2 \cdot 4H_2O$ solution was added drop by drop with a syringe while stirring. Following this addition, the solution was milky white indicating that $MnCO_3$ had been synthesized. The stirring was stopped and the microparticles were left at room temperature for 15 minutes before being washed three times with deionized water. The first supernatant was kept for NMR analysis.

2.7.2. Loading by diffusion in HA-Mn-SM

30 mg of the HA-Mn-SM and 10 mg of TOC were suspended in 5 mL of deionized water and stirred for 24 hours. After 24 hours, the microparticles were washed three times with deionized water. The centrifugation used for this step was 4500 rpm for one minute. The supernatants before and after the first washing were kept for NMR analysis.

2.7.3. Release studies of HA-Mn-SM

For the release studies the same procedure that was used to study the effect of lactic acid on the HA-Mn-SM microparticles was followed. Lactic acid was changed every five minutes and the supernatant was collected, freeze-dried and resuspended in DMSO. The amount of released TOC was analyzed using NMR.

2.8. ROS scavenging effect of the HA-Mn-SM

A fluorometric Hydrogen Peroxide Assay Kit was used to assess the scavenging effect of the microparticles' towards H_2O_2. The concentrations tested were 50, 100 and 250 µg/mL for the microparticles and 50, 100 and 1000 µM for H_2O_2. The calibration curve was developed for 0, 2.5, 5 and 10 µM of H_2O_2.

Three different solutions of the cross-linked HA-Mn-SM 100, 200 and 500 µg/mL and three different solutions of H_2O_2 100, 200 and 1000 µM were prepared in deionized water and mixed in a 1:1 ratio in a final volume of 1 mL. The solutions were shaken for one hour. Then, 50 µL of each solution was added in a 96-well plate duplicate. 50 µL of the buffer was added to each well. This buffer was prepared as per the manufacturer's protocol. The 96-well plate was covered with foil and shaken for a period of twenty minutes before fluorescence values were measured.

2.9. Oxygen generation

0.5 mL of various concentrations of the HA-Mn-SM microparticles solution (50, 100 and 250 µg/mL) were introduced into a vial closed with a septum, using a syringe. While stirring the oxygen, the sensor was immersed in the solution and left for five minutes to equilibrate the oxygen concentration. After five minutes, 0.5 mL of different concentrations of H_2O_2 solution (50, 100 and 1000 µM) were added. The measurements were take over a period of one hour.

2.10. In vitro studies

For the *in vitro* studies, the AlamarBlue® assay was used to check the metabolic activity and the subsequent cytotoxicity of the microparticles on 3T3 rat fibroblasts.

2.10.1. Cell seeding

The cells were cultured in a T75 flask at 37 °C and 5% CO_2 until the population confluency reached 80%. Before seeding the cells into the well plates, the flask was taken out from the incubator and the cells were checked under the microscope for growth and any sign of contamination. The old medium was discarded and replaced by 10 mL of HBSS to rinse cells and remove any traces of medium. The

ACCEPTED MANUSCRIPT

flask was shaken gently and HBSS was discarded. To detach the cells, 3 mL of Trypsin-EDTA was added into the flask which was then incubated for one minute at 37 °C with 5% of CO_2. The flask was shaken and gently tapped to help detach the cells, and checked under the microscope. 7 mL of DMEM was added to deactivate trypsin and then the cells were centrifuged for five minutes at 1200 rpm. The supernatant was discarded and the cells were dispersed in 10 mL of fresh DMEM. 20 µL was collected and placed on the hemocytometer to count cells. The appropriate volume was taken to fill twelve wells with 500 µL of the solution at a final cell concentration of78,125 cells/cm^2. The plates were then placed in the incubator at 37 °C with 5% of CO_2 for 24 hours.

2.10.2. Incubation of the cells with the microparticles

The microparticles were sterilized by resuspension in 70% ethanol overnight, and before use, they were washed twice with HBSS and once with DMEM. Then the microparticles were dispersed in DMEM at concentrations of 50, 100 and 250 µg/mL. The plates were taken out from the incubator and the cells were checked under the microscope for growth and any sign of contamination. The media was then removed and 500 µL of HBSS was added to each well to wash the cells. HBSS was then removed and 500 µL of the desired microparticle solutions were added and placed back in the incubator at 37 °C with 5% CO_2. The metabolic activity of the cells was studied after 24 hours and 72 hours.

2.10.3. AlamarBlue® assay

The plate was taken out from the incubator and the media was removed. The cells were washed once with HBSS. Then, 200 µL of an AlamarBlue® solution, 10% in DMEM, without Phenol Red, was added to each well. Control samples in wells not seeded with cells with AlamarBlue® only and DMEM without phenol red only were also studied. The plate was protected from light using foil and incubated at 37 °C with 5% CO_2 for 4 hours. Then, the solutions from the 48-well plates were transferred to a 96-well plate, 100 µL in each well, and the absorbance was read at 570 nm and 600 nm. The percentage of AlamarBlue reduction was calculated using the following equations:

$$\%\text{AlamarBlue reduction} = (A_{LW} - (A_{HW} \times R_0)) \times 100 \quad \textbf{(Eq. 1)}$$

Where A_{LW} is the absorbance at a low wavelength, A_{HW} is the absorbance at a high wavelength and R_0 is the correlation factor.

$$R_0 = AO_{LW}/AO_{HW} \quad \textbf{(Eq. 2)}$$

ACCEPTED MANUSCRIPT

3. Results and discussion

3.1. Synthesis of MnO_2 spherical microparticles Mn-SM

The protocol used in this study for the fabrication of the spherical microparticles was a combination of two different procedures. We synthesized the $MnCO_3$ core synthesized using h the protocol reported by Pourmortazavi *et al.* [42] and the conditions reported by Fei *et al.* [43] to obtain MnO_2 by reaction of $MnCO_3$ with $KMnO_4$. The first evidence of the formation of MnO_2 microparticles was the change of colour from white ($MnCO_3$) to dark brown (MnO_2). Formation of MnO_2 microparticles was also supported by the FT-IR spectrum (**Figure 1a**). More specifically, the three characteristic peaks of $MnCO_3$ at 722 cm^{-1}, 861 cm^{-1} and 1392 cm^{-1} correspond to the C-O bond. In **Figure 1b**, these peaks can also be observed but the fourth peak at 472 cm^{-1} that corresponds to the O-Mn-O bond of MnO_2 is also evident. The SEM pictures of the $MnCO_3$ (**Figure S1a** - *see supplementary information*) show that the particles are spherical with a diameter that ranges from 0.85 μm to 1.13 μm. **Figure S1b** (*see supplementary information*) shows that the transformation of $MnCO_3$ to MnO_2 does not affect the shape or the size of the particles but changes the surface morphology. Additional evidence of the presence of MnO_2 was the reduction of the ζ-potential from +16.17 ± 6.42 mV to +10.37 ± 5.80 mV (**Table S1)** (*see Supplementary information*).

It is known that MnO_2 reacts with H_2O_2 resulting in the synthesis of H_2O, O_2, and Mn^{2+} in accordance with the following equation 3:

$$MnO_2 + H_2O_2 + 2H^+ \rightarrow 2H_2O + O_2 + Mn^{2+} \qquad \textbf{(Eq. 3)}$$

3.2. Coating with hyaluronic acid and cross-linking using 4-arm-PEG-amine (4S-PEG)

Figure 1c shows the HA-coated microparticles obtained with the second mixture. The surface morphology changed with the appearance of a needle-like material around the particles. Further evidence suggesting a successful coating was the surface charge (ζ-potential) value of our material. Our results (**Table S1**-*see supplementary information*) show that the positive charge of the material was converted into a negative charge, from +10.37 ± 5.80 mV to -37.97 ± 6.21 mV. The change of sign in the ζ-potential can be attributed to the deprotonation of the carboxylic groups contained in each disaccharide of HA [33]. Knowing that HA has a pK_a of around 4 because of these carboxylic groups and that the measurement was carried out at pH 6.5 for the solution used in the coating procedure and 5.5 for the solution used for the measurement of ζ-potential, it is safe to assume that complete deprotonation of the functional group in these conditions has taken place, providing a negative charge to HA. The change of ζ-potential during the coating procedure suggests that HA is bonded to the particles by electrostatic interactions, and these results are consistent with the results obtained by Ravar et al [37]. Another experiment was carried out using 1.80 mL of the NaCl solution and 0.20 mL of HA solution. As these conditions and results are similar to those already presented in this paragraph, they are not presented again here.

During the optimization of the cross-linking procedure, two different buffers (PBS(1X) and MES buffer), as well as two different concentrations of 4S-PEG, 2.5 mg, and 5 mg, were used. The procedure that used PBS(1X) has been excluded due to the presence of large amounts of salts around the particles that could not be completely removed even after numerous washings. As can be observed in **Figure 1d**, when the higher amount of the crosslinker and the MES buffer was used, the morphology of the surface did not change and the spheres kept their original size and shape.

3.3. Effect of lactic acid in the HA-Mn-SM microparticles

To determine the fate of the $MnCO_3$ component in the body and more specifically in an atherosclerotic or inflammatory environment, a dissolution experiment was conducted using lactic acid aiming to stimulate the continuous and overproduction of this type of acid in inflamed cells. After changing the solvent four times, $MnCO_3$ was completely dissolved so removal of this component was not necessary during the synthesis of the platform.

ACCEPTED MANUSCRIPT

In order to check how the coating affects the dissolution of the core and the subsequent release of the loaded TOC, a dissolution test using lactic acid was performed**. Figure 1e** and **1f** shows the result: no spheres can be observed but a needle-like material is present. So, all microparticles are destroyed during the dissolution test. This can be explained by the fact that when $MnCO_3$ is dissolved by lactic acid, the resulting MnO_2 spheres are porous and are not strong enough to keep their shape. This was a good result for the release: the dissolution of $MnCO_3$ allows a controlled release of the encapsulated drug and then MnO_2 can scavenge the ROS. Ultimately, the spheres dissociate and can be easily eliminated by the body.

3.4. Loading and Release studies using with D-α-tocopherol (TOC)

Loading of the HA-Mn-SM was carried out by optimising various parameters including the concentration of TOC during loading, the loading time and the loading method (loading by diffusion and loading by entrapment during the synthesis of the core). These parameters were varied to determine the optimal loading conditions for the D-<alpha>-tocopherol (vitamin-E, TOC). These experiments identified the optimal conditions for TOC loading to be a TOC concentration of 2 mg/mL, a loading time of 24 hours, and loading utilising the diffusion method. Loading by entrapment led to very low encapsulation efficiencies and loading utilising the diffusion method for more than 24 hours did not significantly increase the encapsulation efficiency (data not presented). Lower concentrations of TOC resulted in lower loading efficiency which is attributed to the loss of the material during the washing steps. Furthermore, loading by entrapment during the synthesis of the microparticles was less effective than loading by diffusion which was attributed to the high porosity of the microparticles which rendered them unable to entrap the loaded molecules. On the other hand, coating with HA increased the electrostatic interactions and formed a barrier around the microparticles which limited the capacity of the loaded molecules encapsulated by diffusion to be released. **Figure 2a** reproduced below illustrates that the encapsulation efficiency of TOC was approximately 60% under the conditions described above.

The release studies were conducted using lactic acid at a concentration of 10 mM. The microparticles were treated with 10 mM lactic acid and the lactic acid solution was added every 5 minutes. The lactic acid solution was changed in order to mimic the continuous production of lactic acid which occurs in atherosclerotic tissues and to maintain a stable pH (the pH would change due to the dissolution of $MnCO_3$ after its reaction with lactic acid).

The results from the release studies are presented in **Figure 2b,** which demonstrated that controlled release of TOC occurs in a lactic acid concentration dependent manner. It should be noted that the lactic acid concentration is the cumulative concentration that results from the addition of a new lactic acid solution every 5 minutes. The higher release profile observed after 20 minutes and 3 additions of the lactic acid solution (cumulative 40 mM lactic acid) was approximately 70%. A release study was also performed using the HA-Mn-SM in the presence of 10mM lactic acid over a period of 24 hours. The results demonstrated that the release of TOC was approximately 10%. This result demonstrated that TOC was not released over time, but only in the presence of a high concentration of lactic acid.

3.5. ROS scavenging effect on Hydrogen Peroxide H_2O_2

The scavenging ability of the microparticles is presented in **Figure 3**. It is important to note that even at the lowest concentration of microparticles (50 μg/mL), the particles reduced the concentration of H_2O_2 from 1000 μM to just 60 μM. When the concentration of the microparticles was increased, the scavenging effect was more pronounced. The optimal results were obtained for 250μg/mL microparticles which in the presence of 1000 μM H_2O_2 scavenged almost all of the H_2O_2.

The results presented in Figure 3 demonstrate a dose-dependent scavenging effect since the percentage of H_2O_2 scavenged is increased when the HA-Mn-SM concentration is increased. In addition, given that H_2O_2 is continuously produced in inflamed tissues, our results demonstrate that 50 μg/mL of microparticles are capable of scavenging continuously produced H_2O_2 up to a concentration of 1000 μM, a characteristic that demonstrates the sustained therapeutic effect of the HA-Mn-SM microparticles.

ACCEPTED MANUSCRIPT

3.6. Oxygen generation

As mentioned previously, the reaction of MnO_2 with H_2O_2 produces water and oxygen, thus it was important to assess the generation of oxygen. **Figure 4** shows the results obtained for the measurement of oxygen and **Table S2** (*see Supplementary information*) presents the conditions corresponding to every curve. The generation of oxygen can clearly be observed. The higher curve in graph b - which corresponds to a concentration of 250 µg/mL of microparticles that reacts with a concentration of 1000 µM represents an increase of 6% while the other curves demonstrate a lower increase, of about 1%. This difference may be because the vial volume is very small, so with this amount of microparticles and H_2O_2, the molecules come very quickly into contact leading to more reactions and thereby a higher production of oxygen. This graph demonstrates that we can control the generation of oxygen by controlling the amount of the microparticles that we use. Further *in vitro* and *in vivo* experiments need to be carried out to determine the optimal concentration of microparticles since a low concentration will have no effect on inflamed tissues and a high concentration may lead to unwanted results.

3.7. In vitro studies

In vitro studies have been performed by evaluating the metabolic activity of 3T3 rat fibroblasts using the AlamarBlue® assay. **Figures 5a** to **5d** show the cells alone and the cells with the different concentrations of HA-Mn-SM just after their incubation. As the ROS scavenging effect and the generation of oxygen were assessed for three different concentrations of microparticles, the same concentrations were used for these experiments to ascertain if they have a negative effect on cells. The dose response presented in **Figure 5e** shows that the microparticles did not cause a significant reduction in the metabolic activity for concentrations up to 250 µg/mL and an exposure time of 72 hours indicating that the microparticles are not cytotoxic. A small reduction in the metabolic activity when the concentration of the microparticles was 250 µg/mL was observed compared to lower concentrations but this change is not significant as it resulted after analyzing the data using one-way ANOVA.

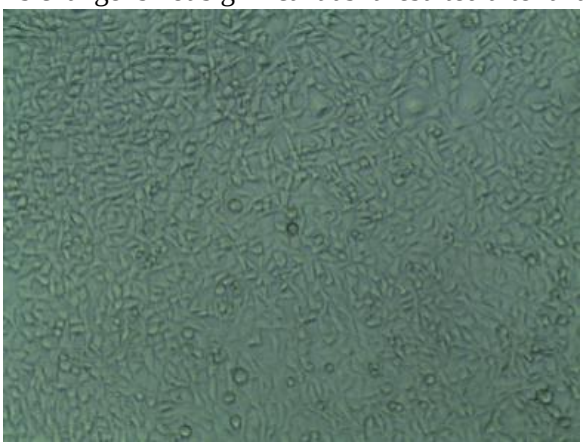

a

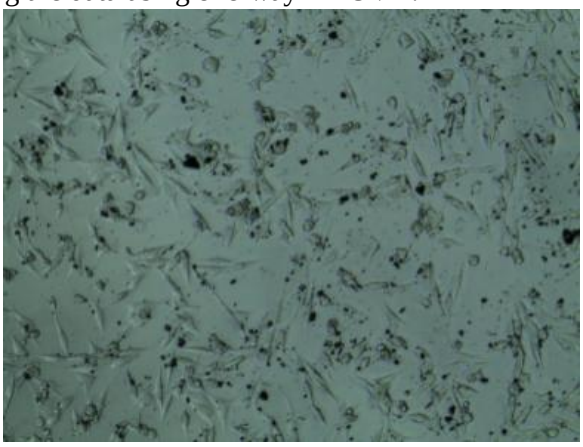

b

ACCEPTED MANUSCRIPT

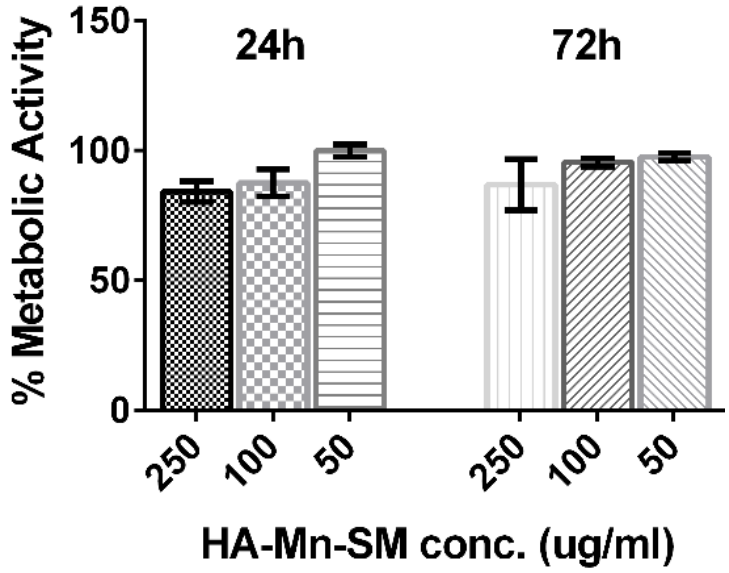

c

Figure 5 : Optical microscopy pictures of 3T3 fibroblastic cells **a)** without microparticles and **b)** with microparticles at a concentration of 100 mg/mL; **c)** percentage of the metabolic activity of 3T3 fibroblasts after treatment with various concentrations of HA-Mn-SM after 24 and 72 hours (one-way ANOVA, n=3, no significant difference).

4. Conclusion

In this study, spherical microparticles with a core-shell structure and an average diameter of 1 µm were synthesized. The microparticles were comprised of a $MnCO_3$ and MnO_2 core and a shell of hyaluronic acid. The fabricated delivery platform was loaded with D-α-tocopherol, that was used as a model 'drug', and the loading and release studies of TOC demonstrated a controlled release profile of the HA-Mn-SM which was lactic acid concentration dependant. The *in vitro* studies didn't reveal any toxicity for up to 72 hours, and the microparticles exhibited a high scavenging ability towards H_2O_2 in addition to the controlled generation of O_2. In addition, given that H_2O_2 is continuously produced in inflamed tissues, our results demonstrate that 50 µg/mL of microparticles are capable of scavenging continuously produced H_2O_2 up to a concentration of 1000 µM, a characteristic that demonstrates the sustained therapeutic effect of the HA-Mn-SM microparticles. These preliminary results indicate the potential use of HA-Mn-SM as a novel platform for the treatment of atherosclerosis.

Acknowledgment

This material is based upon works supported by the European Union funding under the 7th Framework Programme under Grant Agreement Number 317304.

This publication has emanated from research supported in part by a research grant from Science Foundation Ireland (SFI) and is co-funded under the European Regional Development Fund under Grant Number 13/RC/2073. The authors would like to thank Mr Maciej Doczyk for assistance with graphics and Mr Anthony Sloan and Mr Keith Feerick for editorialassistance.

ACCEPTED MANUSCRIPT

Table of Figures

ACCEPTED MANUSCRIPT

References

[1] P. Libby, P.M. Ridker and A. Maseri, Circulation, 105 (2002) 1135.
[2] R. Paoletti, A.M. Gotto and D.P. Hajjar, Circulation, 109 (2004) III.
[3] T.A. Pearson, S.N. Blair, S.R. Daniels, R.H. Eckel, J.M. Fair, S.P. Fortmann, B.A. Franklin, L.B. Goldstein, P. Greenland, S.M. Grundy, Y. Hong, N.H. Miller, R.M. Lauer, I.S. Ockene, R.L. Sacco, J.F. Sallis, S.C. Smith, N.J. Stone and K.A. Taubert, Circulation, 106 (2002) 388.
[4] S.C. Smith, J. Allen, S.N. Blair, R.O. Bonow, L.M. Brass, G.C. Fonarow, S.M. Grundy, L. Hiratzka, D. Jones, H.M. Krumholz, L. Mosca, R.C. Pasternak, T. Pearson, M.A. Pfeffer and K.A. Taubert, Circulation, 113 (2006) 2363.
[5] E.E. Comission, Health statistics - Atlas on mortality in the European Union, 2009.
[6] D. Mozaffarian, E.J. Benjamin, A.S. Go, D.K. Arnett, M.J. Blaha, M. Cushman, S.R. Das, S.d. Ferranti, J.-P. Després, H.J. Fullerton, V.J. Howard, M.D. Huffman, C.R. Isasi, M.C. Jiménez, S.E. Judd, B.M. Kissela, J.H. Lichtman, L.D. Lisabeth, S. Liu, R.H. Mackey, D.J. Magid, D.K. McGuire, E.R. Mohler, C.S. Moy, P. Muntner, M.E. Mussolino, K. Nasir, R.W. Neumar, G. Nichol, L. Palaniappan, D.K. Pandey, M.J. Reeves, C.J. Rodriguez, W. Rosamond, P.D. Sorlie, J. Stein, A. Towfighi, T.N. Turan, S.S. Virani, D. Woo, R.W. Yeh and M.B. Turner, Circulation, 133 (2016) e38.
[7] P.D. Thompson, D. Buchner, I.L. Piña, G.J. Balady, M.A. Williams, B.H. Marcus, K. Berra, S.N. Blair, F. Costa, B. Franklin, G.F. Fletcher, N.F. Gordon, R.R. Pate, B.L. Rodriguez, A.K. Yancey and N.K. Wenger, Circulation, 107 (2003) 3109.
[8] S.C. Smith Jr, S.N. Blair, R.O. Bonow, L.M. Brass, M.D. Cerqueira, K. Dracup, V. Fuster, A. Gotto, S.M. Grundy, N.H. Miller, A. Jacobs, D. Jones, R.M. Krauss, L. Mosca, I. Ockene, R.C. Pasternak, T. Pearson, M.A. Pfeffer, R.D. Starke and K.A. Taubert, J. Am. Coll. Cardiol., 38 (2001) 1581.
[9] M.R. Law, N.J. Wald and A.R. Rudnicka, BMJ, 326 (2003) 1423.
[10] S.J. Nicholls, E.M. Tuzcu, I. Sipahi, A.W. Grasso, P. Schoenhagen, T. Hu, K. Wolski, T. Crowe, M.Y. Desai, S.L. Hazen, S.R. Kapadia and S.E. Nissen, JAMA-J. Am. Med. Assoc. , 297 (2007) 499.
[11] S.-H. Do, B. Batchelor, H.-K. Lee and S.-H. Kong, Chemosphere, 75 (2009) 8.
[12] M.A. Hasan, M.I. Zaki, L. Pasupulety and K. Kumari, Appl. Catal. A-Gen., 181 (1999) 171.
[13] L. Zhang, Z. Fang, Y. Ni and G. Zhao, Int. J. Electrochem. Sci, 4 (2009) 407.
[14] W. Zhang, H. Wang, Z. Yang and F. Wang, Colloid Surface A, 304 (2007) 60.
[15] H. Zhou, Y.F. Shen, J.Y. Wang, X. Chen, C.-L. O'Young and S.L. Suib, J. Catal., 176 (1998) 321.
[16] X.-L. Luo, J.-J. Xu, W. Zhao and H.-Y. Chen, Biosens. Bioelectron., 19 (2004) 1295.
[17] J.A. Roth, Biol. Res., 39 (2006) 45.
[18] J. Varani, I. Ginsburg, D.F. Gibbs, P.S. Mukhopadhyay, C. Sulavik, K.J. Johnson, J.M. Weinberg, U.S. Ryan and P.A. Ward, Inflammation, 15 (1991) 291.
[19] C. Tapeinos, E.K. Efthimiadou, N. Boukos and G. Kordas, Colloids Surf B Biointerfaces, 148 (2016) 95.
[20] E.K. Efthimiadou, C. Tapeinos, A. Chatzipavlidis, N. Boukos, E. Fragogeorgi, L. Palamaris, G. Loudos and G. Kordas, Int J Pharm, 461 (2014) 54.
[21] E.K. Efthimiadou, C. Tapeinos, L.A. Tziveleka, N. Boukos and G. Kordas, Mater Sci Eng C Mater Biol Appl, 37 (2014) 271.
[22] X. Yang, D. He, X. He, K. Wang, Z. Zou, X. Li, H. Shi, J. Luo and X. Yang, Part. Part. Syst. Char., 32 (2015) 205.
[23] Y. Chen, D. Ye, M. Wu, H. Chen, L. Zhang, J. Shi and L. Wang, Adv. Mater., 26 (2014) 7019.

ACCEPTED MANUSCRIPT

[24] C.R. Gordijo, A.Z. Abbasi, M.A. Amini, H.Y. Lip, A. Maeda, P. Cai, P.J. O'Brien, R.S. DaCosta, A.M. Rauth and X.Y. Wu, Adv. Funct. Mater., 25 (2015) 1858.
[25] P. Prasad, C.R. Gordijo, A.Z. Abbasi, A. Maeda, A. Ip, A.M. Rauth, R.S. DaCosta and X.Y. Wu, ACS Nano, 8 (2014) 3202.
[26] C. Tapeinos, A. Larranaga, J.R. Sarasua and A. Pandit, Nanomedicine, (2017).
[27] H.-q. Liu, X.-l. Yu, B. Cai, S.-j. You, Z.-b. He, Q.-q. Huang, L. Rao, S.-s. Li, C. Liu, W.-w. Sun, W. Liu, S.-s. Guo and X.-z. Zhao, Appl. Phys. Lett., 106 (2015) 093703.
[28] M.F. Bennewitz, T.L. Lobo, M.K. Nkansah, G. Ulas, G.W. Brudvig and E.M. Shapiro, ACS Nano, 5 (2011) 3438.
[29] H.B. Na, J.H. Lee, K. An, Y.I. Park, M. Park, I.S. Lee, D.H. Nam, S.T. Kim, S.H. Kim, S.W. Kim, K.H. Lim, K.S. Kim, S.O. Kim and T. Hyeon, Angew Chem Int Ed Engl, 46 (2007) 5397.
[30] J. Huang, J. Xie, K. Chen, L. Bu, S. Lee, Z. Cheng, X. Li and X. Chen, Chem Commun (Camb), 46 (2010) 6684.
[31] D. Pan, S.D. Caruthers, G. Hu, A. Senpan, M.J. Scott, P.J. Gaffney, S.A. Wickline and G.M. Lanza, J Am Chem Soc, 130 (2008) 9186.
[32] N. Li, W. Diao, Y. Han, W. Pan, T. Zhang and B. Tang, Chemistry, 20 (2014) 16488.
[33] L.B. J. Necas, P. Brauner, J. Kolar, Vet. Med.-CZECH 53 (2008) 397.
[34] A. Almalik, S. Karimi, S. Ouasti, R. Donno, C. Wandrey, P.J. Day and N. Tirelli, Biomaterials, 34 (2013) 5369.
[35] G.Y. Lee, J.-H. Kim, K.Y. Choi, H.Y. Yoon, K. Kim, I.C. Kwon, K. Choi, B.-H. Lee, J.H. Park and I.-S. Kim, Biomaterials, 53 (2015) 341.
[36] M.A. Kalam, Int. J. Biol. Macromol., 89 (2016) 127.
[37] F. Ravar, E. Saadat, M. Gholami, P. Dehghankelishadi, M. Mahdavi, S. Azami and F.A. Dorkoosh, J. Control Release, 229 (2016) 10.
[38] X.-y. Yang, Y.-x. Li, M. Li, L. Zhang, L.-x. Feng and N. Zhang, Cancer Lett., 334 (2013) 338.
[39] M. Meydani, J. Nutr., 131 (2001) 366S.
[40] C. Tapeinos and A. Pandit, Adv Mater, 28 (2016) 5553.
[41] P. Bozaykut, B. Karademir, B. Yazgan, E. Sozen, R.C.M. Siow, G.E. Mann and N.K. Ozer, Free Radical Bio. Med., 70 (2014) 174.
[42] S.M. Pourmortazavi, M. Rahimi-Nasrabadi, A.A. Davoudi-Dehaghani, A. Javidan, M.M. Zahedi and S.S. Hajimirsadeghi, Mater. Res Bull., 47 (2012) 1045.
[43] J.B. Fei, Y. Cui, X.H. Yan, W. Qi, Y. Yang, K.W. Wang, Q. He and J.B. Li, Adv. Mater., 20 (2008) 452.

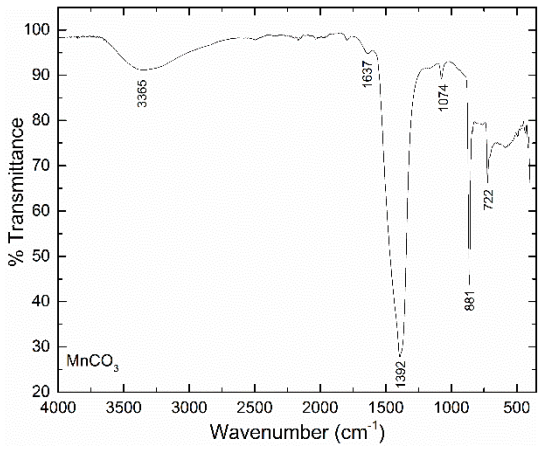

a

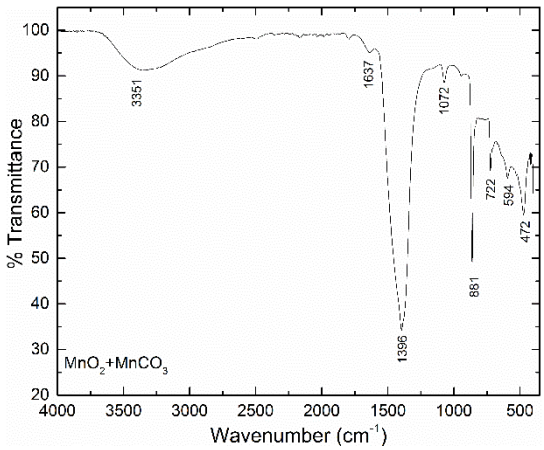

b

ACCEPTED MANUSCRIPT

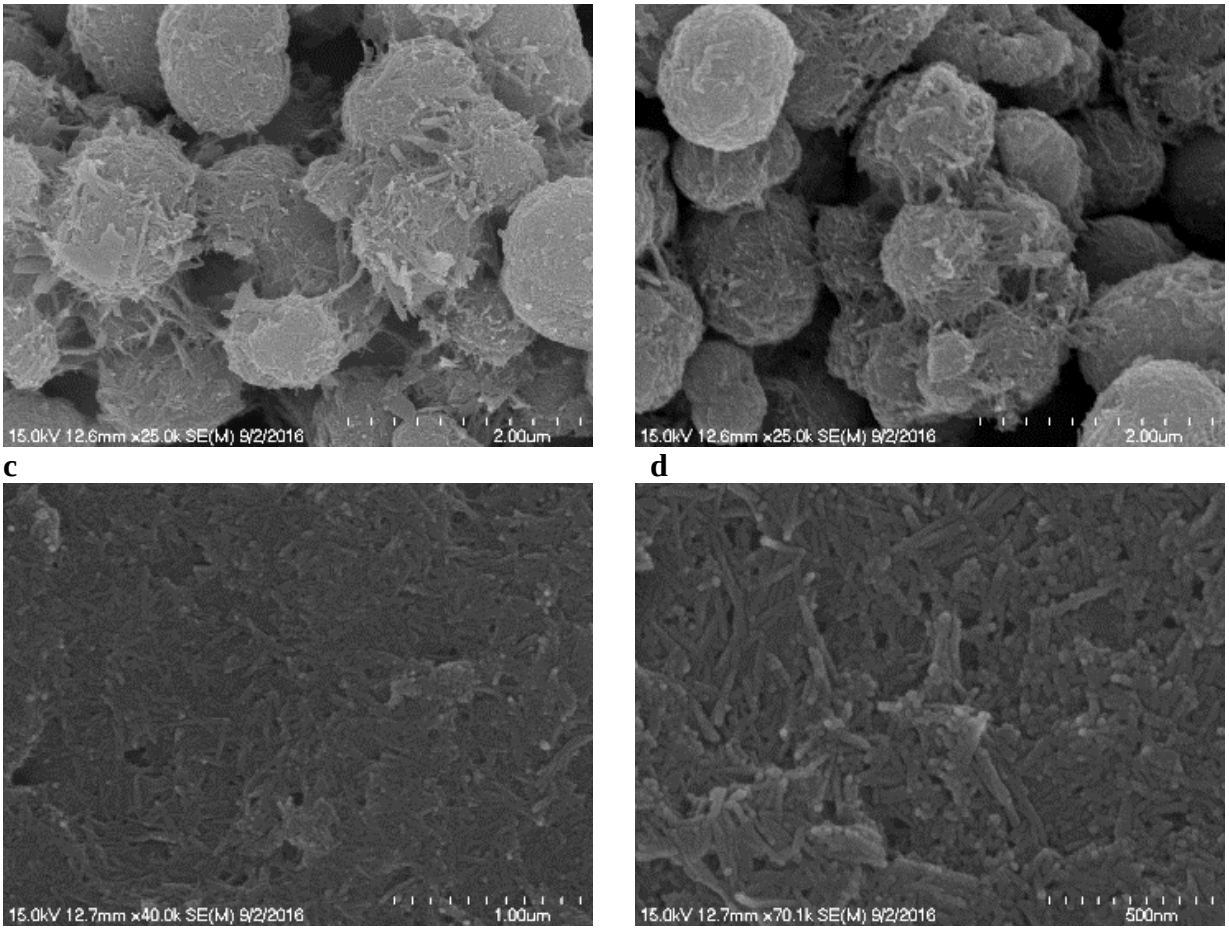

c **d**

e **f**

Figure 1 : FTIR spectrum of **a)** $MnCO_3$ and b) $MnCO_3$+MnO_2 microparticles (Mn-SM); SEM pictures of **c)** $MnCO_3$ microparticles, **d**) Mn-SM microparticles, **e)** HA-Mn-SM, **d)** HA-Mn-SM after the cross-linking, and **e)** and **f)** crosslinked HA-Mn-SM after their dissolution using lactic acid.

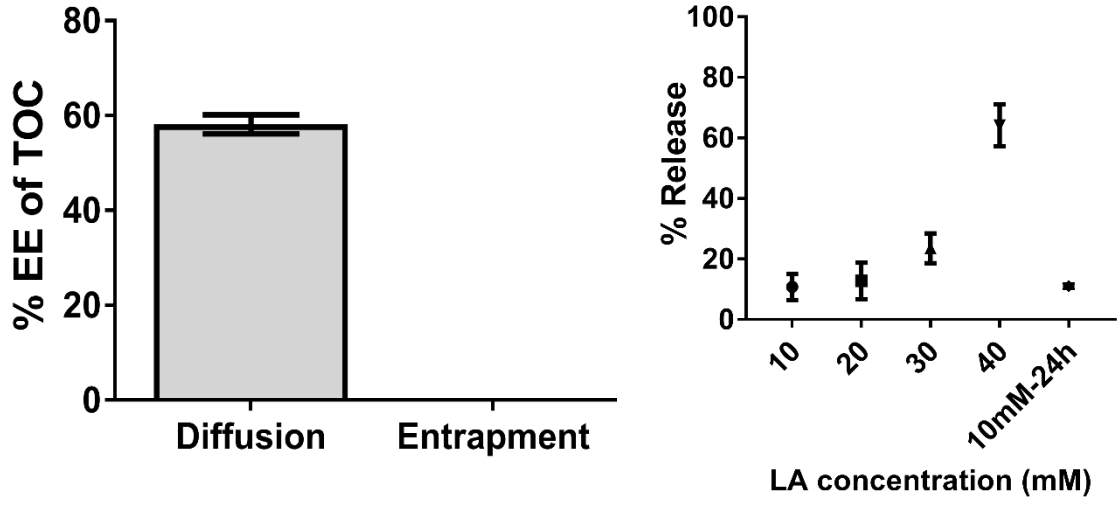

a **b**

Figure 2 : a) % Encapsulation efficiency of the loaded TOC through diffusion and entrapment methods using a concentration of 2 mg/mL and **b)** release studies of TOC after treatment with

ACCEPTED MANUSCRIPT

lactic acid (LA). The lactic acid was changed every five minutes with a fresh addition of lactic acid in order to maintain a pH value of 3. The concentration on the x axis is the cumulative lactic acid concentration after each change. The data were presented as the mean ± SD (n=3).

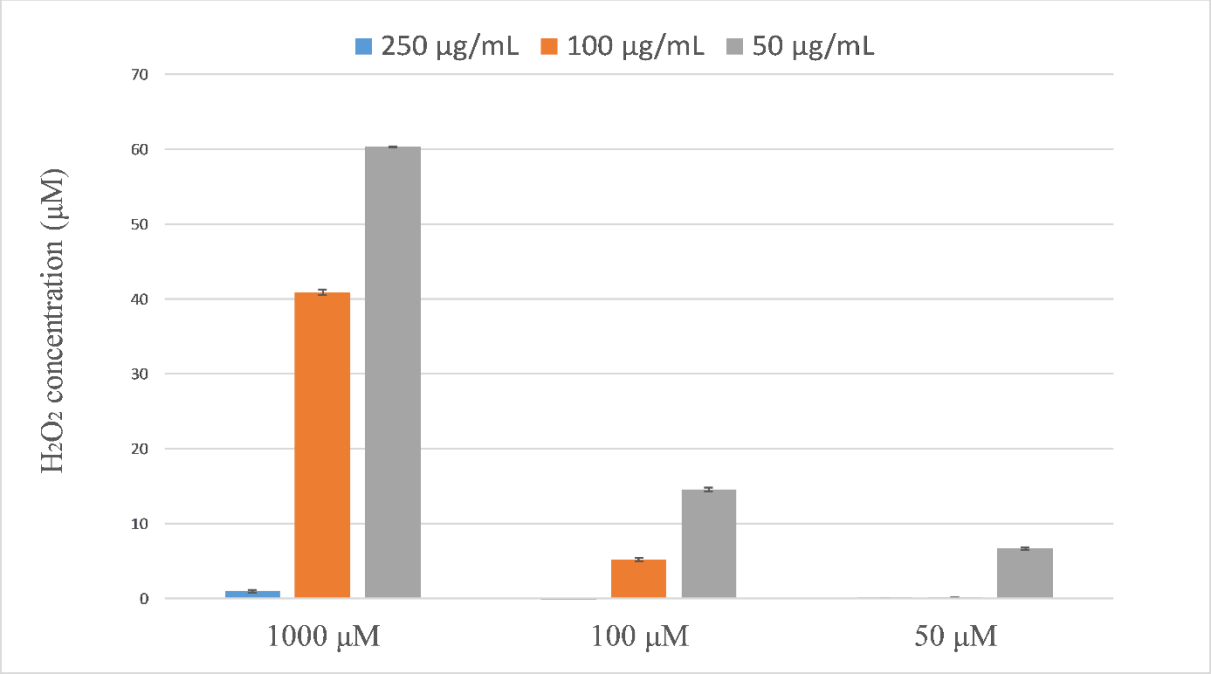

Figure 3 : Concentration of H_2O_2 (50 uM, 100 uM and 1000uM) after incubation with HA-Mn-SM microparticles for 15 minutes at concentrations of 50, 100 and 250 µg/mL Results are presented as mean ± SD (n=2)

b

a

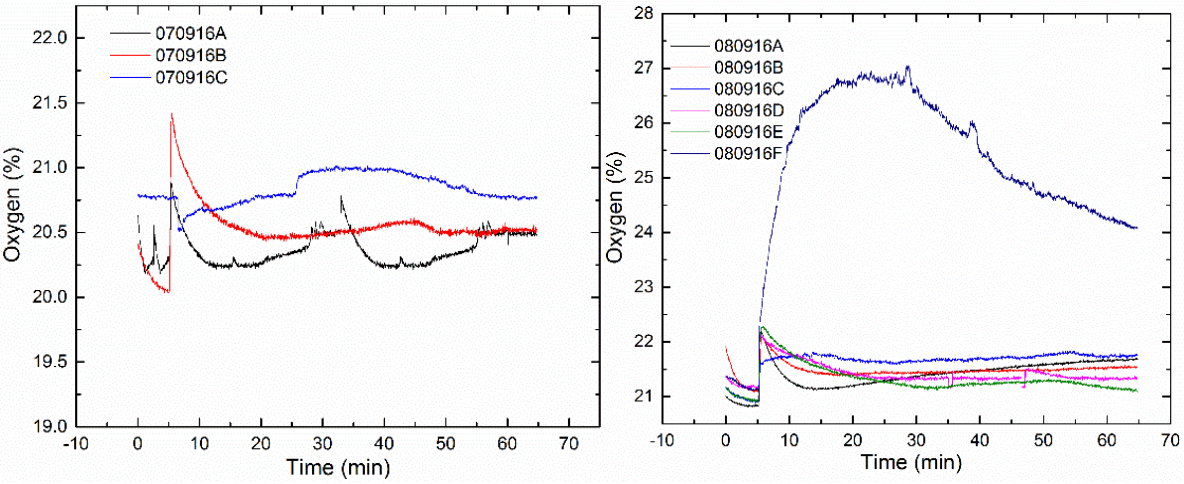

Figure 4 : a) and **b)** The measured amount of generated oxygen as a function of timeusing various amounts of MnO_2 microparticles and various concentrations of H_2O_2. t=5 minutes

ACCEPTED MANUSCRIPT

corresponds to the addition of H_2O_2 to the microparticles solution. Table S2 (*see Supplementary information*) describes in detail the concentrations used in this experiment.